

Quantitative characterization of the growth and morphological evolution of bicrystalline aluminum thin films

D. H. ALSEM*

National Center for Electron Microscopy, Lawrence Berkeley National Laboratory, USA; Department of Applied Physics, Materials Science, University of Groningen, The Netherlands; Materials Science and Engineering Department, University of California, Berkeley, USA

E. A. STACH

National Center for Electron Microscopy, Lawrence Berkeley National Laboratory, USA; School of Materials Engineering, Purdue University, USA

J. TH. M. DE HOSSON

Department of Applied Physics, Materials Science, University of Groningen, The Netherlands

A quantitative and predictive understanding of morphological evolution and mechanical behavior of metallic thin films is necessary for successful processing of electronic devices. Studying idealized thin film systems allows one to gain general insights that can be applied to similar systems. Aluminum (Al) thin films are widely used in electronic applications, in magnetic and optical devices and in coatings, and thus represent an excellent model system.

This letter describes initial observations of the evolution of morphology in mazed Al bicrystal films during deposition and post-deposition annealing. It is known that during annealing, grain growth will occur to reduce the overall system energy, including contributions from strain, grain boundary curvature, and surface and interface energy [1]. Due to the large thermal expansion mismatch, significant compressive stresses develop as the temperature increases. Also, surface self-diffusion may result in grain boundary grooving [2], which may impede further grain growth. Here, we have used *in situ* transmission electron microscopy (TEM) in combina-

tion with automated image analysis tools for grain size determination. Additionally, the film surface at grain boundaries was studied by atomic force microscopy (AFM).

When Al is physical vapor deposited on (100) oriented single crystal silicon (Si) at 280 °C it grows heteroepitaxially [3–5], forming a mazed (110) oriented bicrystal, as per the second-order Potts model [5, 6]. The Potts model describes the ordering of grains in a thin film in two-planar dimensions. The order of the model (Q) determines the number of different grain orientations and therefore limits the tiling of grains within the plane to certain sequences. A first-order ($Q = 1$) Potts Model film is a single crystal without grain boundaries, a second-order ($Q = 2$) film is a mazed bicrystal with grain boundaries (but no triple points present and only two different grain orientations), and $Q = n$ denotes a general polycrystalline film.

Bicrystal Al thin films with thicknesses of 100, 300 and 500 nm on 330 nm (100) Si were prepared by

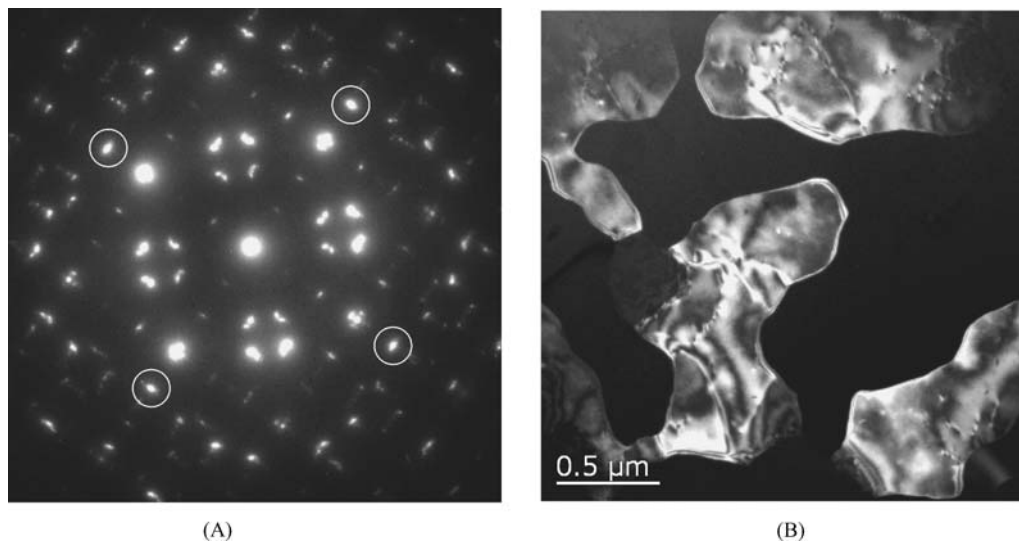


Figure 1 Diffraction pattern (A) and typical two beam dark field image of Al (110) on Si (100) (B). The (02-2) and (0-2-2) spots from both Al orientations are marked by circles in the diffraction pattern.

* Author to whom all correspondence should be addressed.

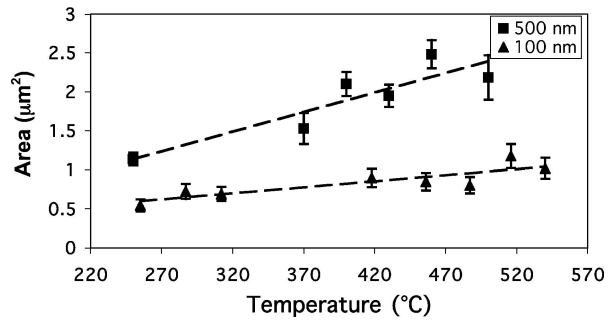
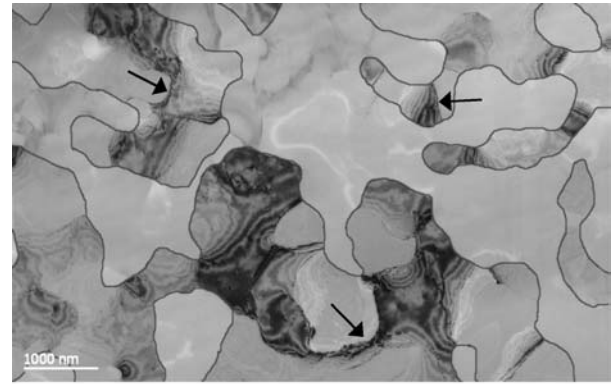


Figure 2 Results of measured grain area during annealing for two (110) Al on (100) Si films. For clarity the data points at room temperature are not shown in the graph.

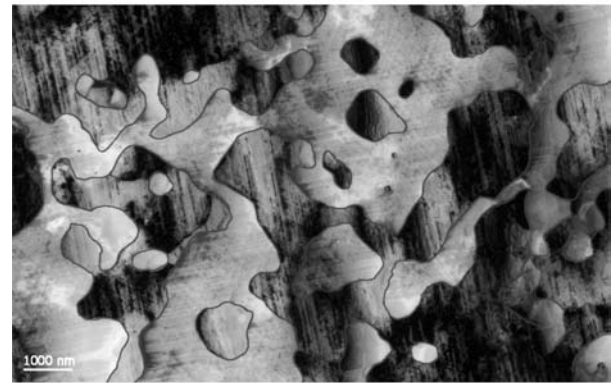
physical vapor deposition (PVD) onto Si SIMOX substrates (330 nm Si (100) on 370 nm SiO₂ on a Si (100) handle layer) at 280 °C at pressures lower than 5×10^{-7} mbar. TEM samples were prepared by chemically etching the Si handle wafer and SiO₂ from the back of the wafer, using standard planar-view Si preparation techniques [7].

TEM diffraction patterns (Fig. 1A), show the different grain orientations in the Al and Si [3]. By selecting the (220) Al diffraction spot in a two-beam, dark-field imaging condition an almost perfect black and white contrast can be achieved (Fig. 1B). Because nearly binary images of the grains can be obtained, it is possible, with some manual retouching, to extract quantitative area data from the images using image-processing tools [8]. The extent of grain boundary grooving was determined using AFM. Fiduciary marks were made on the surface of a 300 nm thick Al bicrystal film using a dual beam focused ion beam (DBFIB) system. The adjacent area was analyzed with an AFM following annealing at elevated temperature to investigate the extent of grain boundary grooving.

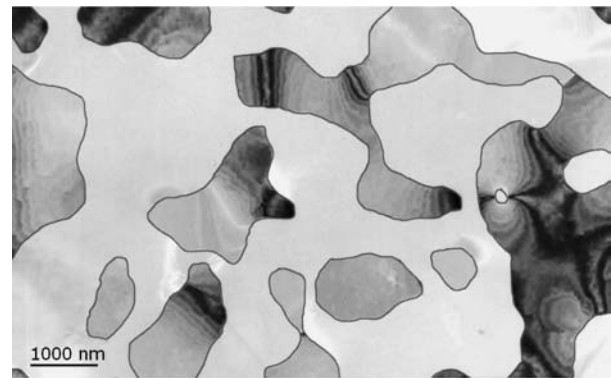
Measured grain area (i.e., average visible grain size) during annealing from 250 to 550 °C (at 577 °C the film/substrate system degenerates) is plotted against the temperature in Fig. 2. The films were annealed inside the TEM. For each temperature data point the films were heated to a certain temperature over the course of ~1 min and kept there for 10–15 min, generally to the point where no further grain boundary motion was observed. The errors are determined by looking at the effect of the image sample size from which the grain areas are extracted, usually tens of grains per data point. Other influences on the magnitude of the errors can be neglected with respect to the effect of the sample size. Measurements of the grain area at room temperature are not shown in Fig. 2, but do not differ significantly from the grain areas measurements at 250 °C. From these results several conclusions can be drawn. There is linear grain growth during annealing of the films and the slope for the different films increases with film thickness ($1.5 \times 10^{-3} \mu\text{m}^2/\text{°C}$ for a 100 nm film and $5.0 \times 10^{-3} \mu\text{m}^2/\text{°C}$ for a 500 nm film). Furthermore, the thicker films had an as-deposited grain size approximately twice as large as observed in the thinner films. This last observation was qualitatively expected from what is known from the literature [1].



(A)



(B)



(C)

Figure 3 A 300 nm bicrystal Al film on 330 nm Si (100) at 550 °C during the first (A) anneal; at room temperature after the first anneal (B) and at 550 °C during the second anneal (C). Inside the two different grain orientations a lot of different sub-grains are present during the first anneal. During cooling down the sub-grains, typical examples are pointed out in (A), have disappeared, but a dense array of dislocations is introduced throughout the entire film. On reheating these dislocations disappear, leaving only bend contours visible inside the grains. Grain boundary in all images have been outlined.

The surface roughness at grain boundaries was measured to be ~20 nm and did not significantly change after annealing up to 400 °C. This suggests that grain boundary grooving is not significant at these temperatures and therefore does not limit grain growth in these films. This is consistent with the fact that the grain size increases linearly until the system decomposes at 577 °C.

An interesting phenomenon was observed during secondary annealing. After cooling the sample to room temperature following the first anneal, then subsequently re-annealing to 500 °C, we observed what appeared visually to be additional grain growth. However,

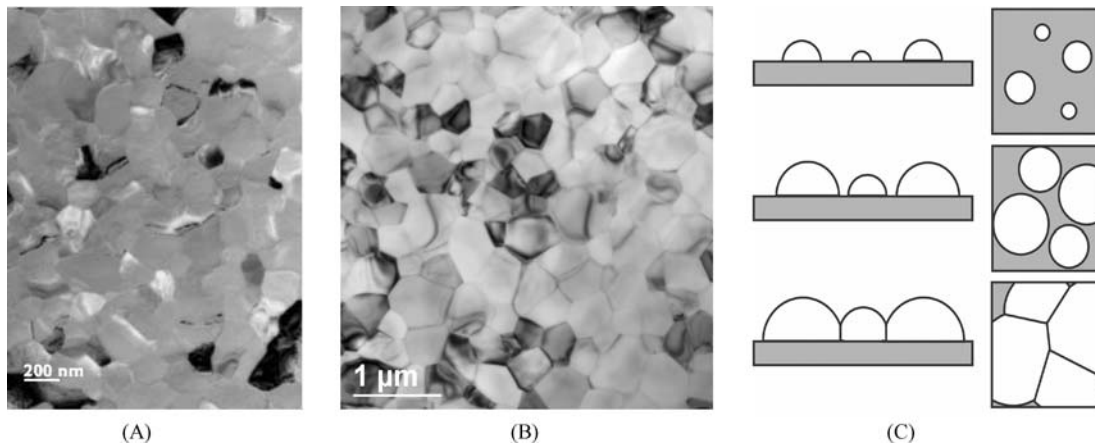


Figure 4 Sub-grains in an as-deposited bicrystal Al film (A) compared to typical poly-crystalline Al film (B). (C) The three stages during film deposition [from 8].

when the images were analyzed quantitatively no statistically significant grain growth was observed. Figs 3A and C show the microstructure of the sample after the first and second annealing cycles respectively. What is apparent in these images is that the sub-grain boundaries (low-angle grain boundaries composed of an array of dislocations) present after the first annealing cycle have disappeared. This disappearance of sub-grain boundaries in the images is what gave the visual impression of additional grain growth. For our grain size measurements, however, the full grain size was measured for all conditions, independent of the presence of sub-grain boundaries.

The formation of these sub-grain boundaries can be explained by considering the similarity between typical bicrystalline Al (Fig. 4A) and polycrystalline Al (Fig. 4B) following deposition. This similarity suggests that these bicrystal films follow a similar growth evolution to polycrystalline films, namely: island formation, island growth and island coalescence (Fig. 4C) [1, 6]. In the case of these bicrystal films, because of the heteroepitaxial nature of the deposition, islands are deposited with one of only two different grain orientations. Thus, upon coalescence, only two types of boundaries may be formed: if the islands are of different orientation, a 90° -angle grain boundary will result. However, if the islands are of the same orientation, the resulting boundary will be a very low angle boundary—i.e., one composed of an array of dislocations that acts to accommodate slight misorientations between the two islands. These small misorientations can increase because additional stresses arise when the island touch upon coalescence [9].

During annealing, it was found that the pre-existing sub-grain boundaries were annihilated. This was a result of the introduction of dislocations into the film during cooling, in order to relieve the tensile thermal misfit strain induced in the film [10, 11]. These dislocations are misfit dislocations which can glide along the $\{111\}$ family of planes, in three directions, namely the $[01-1]$, $[21-1]$ and $[2-11]$ directions. The resulting dense array of thermal misfit dislocations at the film/substrate interface (Fig. 3B) interacted strongly with the dislocations that formed the pre-existing sub-grain boundaries during propagation. These interactions cause the low-

angle grain boundary that divided the sub-grains to be broken up. When the film was annealed a second time, those dislocations that were introduced during cooling were subjected to a compressive stress, causing them to reverse their direction. Because of the presence of the free surface, the thermal misfit dislocations were able to anneal out through the top surface. This eliminated all the dislocations in the film—including those that formed the original sub-grain boundaries (Fig. 3C). At that point, the only contrast remaining in the images is from bend contours. A more detailed description of these dislocation interactions can be found in [11].

It is shown that grain growth in mazed bicrystalline (110) Al thin films on (100) Si can be quantified by setting up a two beam dark field image conditions in a TEM and using image analysis to obtain quantitative information. From this analysis it is shown that linear grain growth occurs during annealing. Thicker Al films differ from thinner films in that they have a larger as-deposited grain size and have a higher grain growth rate. Additionally, we found that in this system grain boundary grooving during annealing was not significant.

Sub-grain boundaries, arrays of dislocation that accommodate small misorientations of growth-islands during film growth, interact with misfit dislocations, introduced upon cooling, after annealing up to high temperatures and annihilate. Upon annealing up to 550°C again these misfit dislocations disappear leaving a more uniform Al microstructure.

Acknowledgements

The authors would like to thank Wouter Soer for his contribution to this letter. The work at the National Center for Electron Microscopy was supported by the Director, Office of Science, Office of Basic Energy Research, Materials Sciences Division of the U.S. Department of Energy under Contract No. DE-AC03-76SF00098.

References

1. C. V. THOMPSON, *Ann. Rev. Mater. Sci.* **30** (2000) 1590.
2. W. W. MULLINS, *J. Appl. Phys.* **28** (1957) 333.

3. N. THANGARAJ, K. H. WESTMACOTT and U. DAHMEN, *Appl. Phys. Lett.* **61**(1) (1992) 37.
4. K. H. WESTMACOTT, S. HINDERBERGER, T. RADETIC and U. DAHMEN, *Mater. Res. Soc. Symp. Proc.* **562** (1999) 93.
5. K. H. WESTMACOTT, S. HINDERBERGER and U. DAHMEN, *Philosoph. Mag. A* **81**(6) (2001) 1547.
6. U. DAHMEN, in "Boundaries and Interfaces in Materials," Proceedings of TMS (1998) 225.
7. E. A. STACH, R. HULL, J. C. BEAN, K. S. JONES, and A. NEJIM, *Microsc. Microanal.* **4**(3) (1998) 294.
8. The Image Processing Toolkit; www.reindeergraphics.com/iptk
9. L. B. FREUND and E. CHASON, *J. Appl. Phys.* **89**(9) (2001) 4866.
10. W. D. NIX, *Metal. Trans. A* **20A** (1989) 2217.
11. E. A. STACH, U. DAHMEN and W. D. NIX, *Mater. Res. Soc. Symp. Proc.* **619** (2000) 27.

*Received 24 November 2004
and accepted 21 March 2005*